Article

Magnetophoretic Transport Line System for Rapid On-Chip Attomol Protein Detection

Rebecca Stjernberg Bejhed, Tian Bo, Kristofer Eriksson, Rimantas Brucas, Sven Oscarsson, Mattias Strömberg, Peter Svedlindh, and Klas Gunnarsson

Langmuir, **Just Accepted Manuscript** • DOI: 10.1021/acs.langmuir.5b01947 • Publication Date (Web): 26 Aug 2015

Magnetophoretic Transport Line System for Rapid On-Chip Attomol Protein Detection

Rebecca S. Bejhed,[†,§] Tian Bo,[†,§] Kristofer Eriksson,[†] Rimantas Brucas,[†] Sven Oscarsson,[‡] Mattias Strömberg,[†] Peter Svedlindh,[†] and Klas Gunnarsson*[,†]

[†]Department of Engineering Sciences, Division of Solid State Physics, The Ångström Laboratory, Uppsala University, Box 534, SE-751 21 Uppsala, Sweden

[‡] Department of Organic Chemistry, Arrhenius Laboratory, Stockholm University, SE-106 91 Stockholm, Sweden

[§] Authors contributed equally to this work

ABSTRACT: A lab-on-a-chip travelling wave magnetophoresis approach for sensitive and rapid protein detection is reported. In this method, a chip-based magnetic microarray comprising lines of micron-sized thin film magnetic elements was used to control the movement of magnetic beads (MBs). The MBs and the chip were functionalized forming a sandwich-type assay. The MBs were transported across a detection area and the presence of target molecules resulted in immobilization of MBs within this area. Target quantification was accomplished by MB counting on the detection area using an optical microscope. In order to demonstrate the versatility of the microarray, biotinylated anti-avidin was selected as the target protein. In this case avidin functionalized MBs and an avidin functionalized detection area were used. With a total assay time of 1 to 1.5 hours (depending on the labelling approach used), a limit of detection in the attomol range was achieved. Compared to on-chip surface plasmon resonance biodetection systems, our method has a larger dynamic range and is about a factor of 500 times more

sensitive. Furthermore, our MB transportation system can operate in any chip-based biosensor platform, thereby significantly improving traditional biosensors.

Keywords: Lab-on-a-Chip Biosensor Device, Travelling Wave Magnetophoresis, Magnetic Beads, Magnetic Thin Films, Protein Detection.

INTRODUCTION

Sensitive and rapid assays for the detection of biomarkers provide essential information regarding e.g. diagnosis and disease management and are thus of large interest in research and clinical applications.[1-2] For nucleic acid biomarker detection, polymerase chain reaction (PCR) and other enzymatic amplification methods have been regarded as the gold standard of today and are utilized in designing sensitive detection platforms.[3] Although amplification strategies to detect protein biomarkers exist, e.g. enzyme linked immunosorbent assay (ELISA), proteins cannot be enzymatically amplified in the same direct manner as nucleic acids (e.g. PCR). This fact further increases the demand for sensitive, specific, rapid and high-throughput methods for protein detection.[4] In order to circumvent this deficiency, the research community has turned to nanoscale and micron-scale labels to improve the limit of detection (LOD) and increase the specificity for the detection of low biomarker concentrations.[5] One type of label, which has gained increased attention during the past decade, [6-8] is magnetic beads (MBs)

MBs can easily be manipulated and separated using magnetic field gradients, which provides a good purification method and strongly facilitates assay protocols.[9] Furthermore, considering the inherently negligible magnetic background of biological objects, MBs require minimal

sample purification and yet achieve a high signal-to-background contrast when being used for labeling.[10] Based on their unique properties, MBs have been used in a number of recently developed magnetic biosensors.[5, 11-17]

Magnetic detection methods could be classified into two groups; volumetric and surface-based.[10] Volumetric methods, such as nuclear magnetic resonance and magnetic relaxation measurements, detect the signal from the entire sample volume. Hence, the loss of signal is small and the assays are fast and simple. Surface-based sensors, on the other hand, can achieve higher sensitivity and resolution by directly detecting individual (magnetic) objects. However, typical large biological analyte molecules can only diffuse 10-100 μm in the minutes-to-hours timescale, leading to a weak or non-existing signal from target far away from the detection area.[18] To address this problem, a lot of effort has been put into transporting and/or binding the target molecules to the sensing elements utilizing different forces such as hydrodynamic,[19-20] electrostatic[21-22] and/or magnetic.[23-26]

Here we describe a magnetophoretic chip-based microarray comprising lines of micron-sized magnetic thin film elements designed to manipulate the movement of MBs. The assay is based on traveling wave magnetophoresis, where a translating periodic magnetic potential energy landscape is used for horizontal transport of MBs.[27-30] This work is based on previous work published by our group describing firstly the controlled motion of MBs,[31] and secondly the possibility of transporting proteins immobilized on MBs.[32] In this continuation, the focus has been on developing an immunoassay using the knowledge gained in previous studies. In this assay, the MBs are magnetically transported across a gold area (the detection area) where both the MBs and the detection area are functionalized with biomolecules complementary to the target biomolecule, thereby forming a sandwich-type assay. Presence of target gives rise to

immobilization of MBs within the detection area and target quantification is accomplished by MB counting on the detection area using a standard optical microscope. The microarray provides a simple detection method for biomolecular interactions, does not require expensive analysis equipment or components and can detect low levels of target molecules with a LOD in the attomol range within a total assay time of 1 to 1.5 hours (depending on the labelling approach used). No electrical wiring in contact with the liquid is required and the need for microfluidic components is kept to a minimum. Furthermore, our MB transportation system can operate in any chip-based biosensor platform such as one using a quartz crystal microbalance (QCM) sensor, thereby improving traditional biosensors as well as providing quantitative results. The functionality of the microarray is proved using avidin functionalized MBs and an avidin functionalized detection area, whereas biotinylated anti-avidin is used as the target antibody.

EXPERIMENTAL SECTION

The set-up. The basic physical mechanism behind the magnetophoretic setup is presented in previous work published by our group,[31] where an external in-plane rotating magnetic field and thin film elliptic magnetic elements are used for transportation of liquid suspended MBs. In the present paper, the MBs are suspended in a buffer solution [10 mM phosphate buffer saline (PBS) with 0.1% Tween-20 and 0.1% bovine serum albumin (BSA), VWR International AB, Sweden]. The buffer solution covers the surface of the transport lines and the detection area. Since unreacted and nonspecifically bound molecules are washed away from the MBs during transportation, the need of a rinsing step before adding the MBs to the transport lines is eliminated. The amount of target molecules in the sample is correlated to the amount of MBs becoming immobilized on the detection area, which is easily detected using a standard low-

magnification optical microscope.[33] A schematic illustration and photographs of the experimental set-up can be seen in Scheme 1. A microchip with rows of elliptical magnetic thin film elements and a gold covered detection area (Scheme 1e) is centrally positioned in a fluid cell comprising a silicon bottom part, a glass top part and a gasket made out of photoresist (Scheme 1b). The bottom part has an inlet and an outlet for the channeling of liquids across the microchip (Scheme 1d). The inlet in this setup is designed for both buffer and MBs injection. The fluid cell is located in the center of two pairs of electromagnets oriented perpendicular with respect to each other and fixed in a supporting platform made out of aluminum (Scheme 1c). In order to transport MBs along the rows of ellipses and across the detection area, a rotating in-plane magnetic field with a magnitude of 20 kA/m and a rotational frequency of 1.3 Hz was applied. The stray field of the magnetized ellipses forces the MBs to move along the rims of the ellipses, following the direction of the rotating field. Every half cycle the MB jumps from the long side of an ellipse to the apex of the neighboring one.[31] The electromagnets are powered by a Hewlett Packard 6626A power supply and controlled using a LabView program. A syphon controlled tubing system was used to administer buffer solution, with or without MBs, into the fluid cell through the inlet. Transportation of MBs was observed using an Olympus BX60 microscope equipped with a 4x-objective and a digital camera capable of video imaging. The snapshots from the uc480Viewer controlled camera recordings were analyzed using the public domain Java image processing software ImageJ.[34-35]

The chip. A Si(100) wafer with a 100 nm thick thermally grown oxide layer was spin coated with a positive photoresist and a pattern of ellipses was transferred to the wafer using a contact lithography process. The ellipses (2.8 μm × 10 μm or 4 μm × 10 μm) were arranged in rows with a 12 μm center-to-center distance to the nearest neighbor and with a 40 μm distance between

parallel rows (cf. Scheme 1e). A 75 nm thick film of the soft magnetic material permalloy, $Ni_{0.8}Fe_{0.2}$, with 10 nm of titanium as adhesion layer was thermally evaporated onto the wafer and the pattern was transferred through a lift-off process using acetone. The wafer was subsequently coated with a second layer of positive photoresist and a pattern consisting of 1.2 mm wide stripes was transferred to the wafer using photolithography. Then, a 10 nm thick gold layer with 10 nm of titanium as adhesion layer was evaporated onto the photoresist and the stripe pattern was transferred through lift-off using acetone. Finally, the wafer was diced into 5×5 mm^2 sized chips, each containing several rows of elliptical permalloy elements and one gold rectangle positioned at the center of the chip. The individual chips were functionalized with capture molecules using a two-step process. Prior to functionalization the chips were exposed to a 1000 W oxygen plasma for one minute, ensuring a clean gold surface. In the first step, 6 µl of 20 mM SH-PEG_{3400}-biotin (Nanocs Inc., USA) in 10 mM PBS, pH 7.5, was pipetted onto each chip. The reaction between the gold and the modified biotin was carried out at room temperature for no less than 24 hours, creating a self-assembled SH-PEG_{3400}-biotin film on the gold surface.[36-37] Secondly, the chips were washed twice with buffer solution after which 5 µl of 0.2 mM avidin (Vector Laboratories Inc., USA) solution was added to each chip. The reaction between biotin and avidin was carried out at 37°C for 30 minutes.

The MBs. Commercially available Micromer®-M MBs (Micromod Partikeltechnologie GmbH, Germany) with an average diameter of 5 µm were used in the experiments. Each MB consists of a core of magnetite (Fe_3O_4) nanocrystals embedded in a styrene-maleic acid-copolymer matrix. The MBs are dispersed in PBS with a concentration of 3.5×10^8 MBs/ml (25 mg/ml of solid content) and have a polymer surface coating with covalently bound avidin

molecules (capture molecules). According to the manufacturer, the protein binding capacity is 450 ng of avidin per mg MBs.

Experimental methods. Two different approaches, cf. Fig. 1, were evaluated with regard to how the target antibody is assayed. In the first approach, denoted the *off-chip labeling approach* (panel a), the MBs were incubated with the antibody before being transported across the chip. In the second approach, denoted the *on-chip labeling approach* (panel b), the antibody was incubated with the chip before the MBs were transported across the chip. In the off-chip labeling approach, Fig. 1a, 2 µl of MBs at a concentration of 25 mg/ml was mixed with 100 µl biotinylated anti-avidin (Vector Laboratories Inc., USA) and left to react for 30 minutes at 37°C. The MBs were then magnetically separated from the solution, resuspended in 40 µl buffer solution and finally injected into the fluid cell harboring the chip. In the on-chip labeling approach, illustrated in Fig. 1b, the avidin functionalized chips were washed twice with buffer solution. 5 µl of biotinylated anti-avidin was then pipetted onto the chip surface followed by incubation for 30 minutes at 37°C. 2 µl of MBs at a concentration of 25 mg/ml was diluted with 38 µl buffer solution after which the diluted MB suspension was injected into the fluid cell harboring the chip. For both approaches, the concentration of biotinylated anti-avidin was varied to generate corresponding dose-response curves.

At the beginning of each experiment, the fluid cell was filled with buffer solution using a syphon. The MB suspension was then added through the tubing system. The magnetic transport was turned on and the syphon controlled flow was turned off. Movements of MBs were then purely governed by the magnetic forces due to the ellipses. Firstly, the MBs were transported through the buffer solution in order to remove any residual nonspecifically bound substances. The MBs were then magnetically transported across the detection area comprising the

functionalized gold rectangle. When the MBs, visible through the microscope, had been given on average 15 seconds to interact with the capture molecules on the detection area, the syphon was turned on. Then, non-specifically bound MBs were rinsed away from the detection area and new MBs were transported across the chip. If the system is to be used for detection of target molecules displaying lower affinity to the capture molecules than the hereby presented system, the MB-detection area interaction time should be increased. The syphon was stopped and the magnetic forces between MBs and magnetic thin film elements once again controlled the movement of the MBs. This was repeated in sequence for the duration of seven minutes, resulting in approximately five minutes of actual interaction time between MBs and detection area.

In either of the labeling approaches, if on the one hand a negative sample is analyzed, nothing will bind to the detection area and MBs will not become immobilized on the chip. If on the other hand, the sample is positive, the target antibodies will act as molecular bridges between the MBs and the detection area in a sandwich manner (avidin – biotinylated anti-avidin – avidin), as can be seen in Fig. 1.

To ensure that MBs did not immobilize due to the remanent magnetization of the permalloy ellipses, the chip was demagnetized after each transport sequence. The demagnetization procedure was performed by applying a step-wise decreasing magnetic field with alternating sign. Finally, the chip was rinsed using a flow of buffer solution. Four images each covering approximately 1600×1200 μm^2 of the detection area were analyzed by the image analysis software.[34-35] The output from the image analysis was the average relative surface coverage of specifically bound MBs in percent of the total detection area, where the relative coverage is equal to the coverage (specific and nonspecific) of the detection area minus the coverage

(nonspecific) outside of the detection area. The calculation of the relative coverage was made under the assumption that the nonspecific binding of MBs per area unit is equal for the entire chip, i.e. both on and outside of the detection area. Based on the result for the blank control sample, this assumption is considered to be reasonably accurate. It was found that the differences between the two surfaces are not significant since the relative coverage of blank controls is close to zero (0.81% and 0.20% for off-chip and on-chip labeling, respectively). Hence, the area outside of the detection area can be used to calculate the background signal generated by nonspecific binding of MBs.

In order to estimate the magnetic force acting on a MB, a tolerance experiment was performed. Using a syringe pump, the MBs were magnetically transported in a controlled counter flow of buffer solution without BSA. At a flow rate of 100 µl/min, the MBs could no longer be transported using the same rotating magnetic field as was used during the assay experiments. The force from the flow of buffer acting on a MB was calculated using Stokes' equation for a small sphere moving through a viscous fluid, $F_D = 6\pi\mu Rv$, where μ is the dynamic viscosity of the fluid, R is the radius of the MB and v is the velocity of the fluid relative to the MB. When using the viscosity for water at room temperature and the nominal radius of a MB (2.5 µm), the resulting Stokes' drag force was equal to 160 pN. Neglecting any weaker forces, such as gravitational, this gives the magnitude of the magnetic force responsible for moving the MBs from one ellipse to the next. The distance one MB has to travel when moving between two ellipses is approximately 1.5 times the MB diameter (cf. Scheme 1e). In a study by Yellen et.al,[38] the magnetic force from a magnetic thin film element acting on a MB was calculated as a function of distance between the two showing that for a distance of 1.5 times the MB diameter, the force on the MB was approximately 350 pN, corroborating our calculations.

Considering that a single 5 μm MB could be bound to the surface via more than one single recognition event, the Stokes' drag force is smaller than the rupture strength of the immunochemical complex (approximately 60–250 pN)[39] or specific DNA duplex (approximately 800–1200 pN),[40] but much larger than weak nonspecific interactions (approximately 0.1–10 pN).[41]

RESULTS AND DISCUSSION

In Fig. 2, photomicrographs, each showing approximately 1270×260 μm^2 of the detection area, displaying surface coverage results are presented. The photomicrographs are cropped versions of experimental results using the on-chip labeling approach. From top to bottom the results are shown for a negative, a slightly positive (target concentration of around 1 ng/ml) and a positive (target concentration of around 1 μg/ml) sample, respectively. Note that the concentration of target antibody is determined from averages of three tests. The total area of each test is approximately 1600×4800 μm^2, i.e., almost 24 times larger than the photomicrograph shown here. Thus, the photomicrographs displayed here are only aiming at providing a direct impression about the coverage, but cannot directly be related to the concentration of the target.

In Fig. 3, the result from measurements performed using the off-chip labeling approach is presented. Using disposable chips, six different concentrations of biotinylated anti-avidin were measured three times each. The average relative surface coverage and standard deviation between three different chips were calculated for each concentration. In Fig. 3, the average surface coverage and standard deviation for each triplicate measurement are plotted versus the concentration of target antibody in pg/ml. The LOD was calculated as the average surface coverage for a triplicate measurement using a blank control sample plus three times the standard

deviation of the triplicate. In Fig. 3, the LOD is represented by a dashed line. Using the off-chip labeling approach the LOD was 100 pg/ml, which corresponds to about 67 attomol of target molecules in the 100 µl sample.

In Fig. 4a, the result of a series of measurements performed using the on-chip labeling approach is presented. The data was processed as described above. As can be seen from the figure, the LOD was 50 pg/ml, which corresponds to 1.7 attomol of target molecules in the 5 µl sample. The total assay time for the on-chip labeling approach was 1.5 hours and the dynamic range proved to be as much as five orders of magnitude. This on-chip labeling approach exhibits a superior LOD as well as shorter analysis time compared to most of the common sandwich assay based protein detection methods,[42] especially when considering that no signal amplification method (such as PCR or enzyme-link) has been employed to improve the sensitivity. The high sensitivity can only be achieved using the magnetic transport lines, which have three main beneficial effects: Firstly, aided by gravity MBs dispersed in the sample volume will come close enough to the chip surface to be attracted by the magnetic force due to the magnetic thin film elements of the transport lines. Once trapped, the forced motion of MBs towards the detection area increases the relative target concentration (only valid for the off-chip approach) and the MB concentration (valid for both approaches) at the detection area. Secondly, due to the forced motion of the MBs, the possibility for the molecules on the MBs to react with the detection area is improved compared to traditional surface-based methods.[23-24, 43-45] Finally, the fluid cell is designed so that the direction of magnetic transport is opposite to the direction of buffer flow. This effect can be used to recover MBs that have been washed or transported across the detection area without becoming immobilized, thereby giving those MBs a second chance to become immobilized on the detection area.

In order to validate the significance of the magnetic field controlled MB transportation, three concentrations of target antibody, ranging from 0.01 mg/ml (highest target concentration in Fig. 4a) to 1 mg/ml, were selected for zero magnetic field measurements using the on-chip approach. The results are presented in Fig. 4b, showing that not even the coverage for the highest concentration (1 mg/ml) is above the LOD previously established. Thus, it can be concluded that the magnetic field controlled MB transportation is a necessary and essential component of the assay.

When comparing the two approaches, it is evident that the off-chip labeling approach is somewhat less sensitive than the on-chip labeling approach which is mainly due to the choice of target molecule. Biotinylated anti-avidin can bridge two MBs and will in such a case be sterically hindered from also interacting with the detection area. Both approaches require an excess of MBs (labels) since many MBs are lost during one experiment. The main reason for the loss of MBs is the comparatively large sample volume needed in the current set-up, only about 5-10% of this volume actively contributes to the experimental results. Upgrading the set-up by constructing separate inlets for the buffer and MB suspension could diminish this loss. For the on-chip labeling approach this is a minor problem resulting only in the loss of MBs. In the case of the off-chip labeling approach, however, this leads to the loss of not only MBs but also target. The reason for this being that the target is bound to the MBs prior to the MBs being injected into the set-up. The total assay time of the off-chip labeling approach is not more than one hour (compared to 1.5 hours for the on-chip labeling approach) since the chip-avidin incubation and MBs-target molecule incubation can be processed in parallel rather than in series. This is much faster than commonly used antibody detection methods such as ELISA, which always takes more than 3-4 hours due to its time-consuming coating (usually performed overnight) and blocking

steps. Apart from the gain in assay time, the off-chip labeling approach has the advantage of easily being combined with MB-based target enrichment in order to create a high throughput assay.

As antibodies are frequently assayed in serum samples, the effect of adding 10% serum (fetal bovine serum, Sigma-Aldrich Sweden AB) to the buffer solution was studied using the on-chip approach. From the results presented in Fig. 4c it can be observed that the LOD increases from 50 pg/ml to 1 ng/ml, i.e. by a factor of 20, which corresponds to approximately 34 attomol of target in a 5 µl sample. We attribute this increase of the LOD mainly to sample matrix effects, e.g., higher sample viscosity and higher nonspecific adsorption. Moreover, the increased LOD may also in part be explained by the fact that serum always contains biotin as well as a background of biotinylated serum proteins causing additional immobilization of MBs on the detection area. Still, the achieved LOD in the presence of serum is well within required limits for the assay to be highly competitive in comparison to already existing assays.

SUMMARY AND CONCLUSION

In summary, we present a lab-on-a-chip approach for sensitive, low-cost, easy and rapid detection of protein targets. Compared to on-chip surface plasmon resonance biodetection systems, our setup has a larger dynamic range and is about a factor of 500 times more sensitive.[46] Further developing this lab-on-a-chip approach, the system could easily be extended for multiplex analysis, e.g., by adding additional detection areas, differently functionalized, and in the same experiment exposing the sample to two or more types of MBs functionalized with different capture molecules. Furthermore, our MB transportation system can operate in any chip-based biosensor platform, thereby significantly improving traditional biosensors. Using the on-

chip labeling approach in combination with the presented image analysis procedure, we have demonstrated a LOD of 50 pg/ml. To further improve the sensitivity, transport lines using smaller magnetic elements, keeping in mind that the size has to be above the magnetic single domain limit, being able to transport nanoscale MBs providing higher surface to volume ratio could be designed. However, changing to smaller MB labels requires replacing the optical lithography used for making the transport lines in the present study with nanolithography capable of producing transport lines with nanoscale dimensions. Also, while the micron-scale MBs used in the present study are visible in a standard low-cost optical microscope, nanoscale MBs will require a different read-out method. One possibility would be to use a QCM sensor for read-out, providing the additional benefit of a quantitative analysis. As for protein detection, the sensitivity of MB enhanced QCM (0.6 pg/ml)[47] may be further improved by utilizing magnetic transport providing a more efficient mass enhancement.

AUTHOR INFORMATION

Corresponding Author

* E-mail: klas.gunnarsson@angstrom.uu.se (K.G).

Notes

The authors declare no competing financial interest.

ACKNOWLEDGMENTS

This work was supported by the Knut and Alice Wallenberg (KAW) Foundation, the Swedish Research Council and Formas (project number 221-2012-444). Junxin Wang is acknowledged for his contribution to the illustrations.

REFERENCES

(1) Hood, L.; Heath, J. R.; Phelps, M. E.; Lin, B. Y. Systems biology and new technologies enable predictive and preventative medicine. *Science* **2004**, *306*, 640-643.

(2) Virgin, H. W.; Todd, J. A. Metagenomics and Personalized Medicine. *Cell* **2011**, *147*, 44-56.

(3) Emmadi, R.; Boonyaratanakomkit, J. B.; Selvarangan, R.; Shyamala, V.; Zimmer, B. L.; Williams, L.; Bryant, B.; Schutzbank, T.; Schoonmaker, M. M.; Wilson, J. A. A.; Hall, L.; Pancholi, P.; Bernard, K. Molecular Methods and Platforms for Infectious Diseases Testing A Review of FDA-Approved and Cleared Assays. *J Mol Diagn* **2011**, *13*, 583-604.

(4) Tekin, H. C.; Gijs, M. A. M. Ultrasensitive protein detection: a case for microfluidic magnetic bead-based assays. *Lab on a Chip* **2013**, *13*, 4711-4739.

(5) Gaster, R. S.; Xu, L.; Han, S. J.; Wilson, R. J.; Hall, D. A.; Osterfeld, S. J.; Yu, H.; Wang, S. X. Quantification of protein interactions and solution transport using high-density GMR sensor arrays. *Nat Nanotechnol* **2011**, *6*, 314-320.

(6) Llandro, J.; Palfreyman, J. J.; Ionescu, A.; Barnes, C. H. W. Magnetic biosensor technologies for medical applications: a review. *Med Biol Eng Comput* **2010**, *48*, 977-998.

(7) Koh, I.; Josephson, L. Magnetic Nanoparticle Sensors. *Sensors-Basel* **2009**, *9*, 8130-8145.

(8) Tamanaha, C. R.; Mulvaney, S. P.; Rife, J. C.; Whitman, L. J. Magnetic labeling, detection, and system integration. *Biosens Bioelectron* **2008**, *24*, 1-13.

(9) Borlido, L.; Azevedo, A. M.; Roque, A. C. A.; Aires-Barros, M. R. Magnetic separations in biotechnology. *Biotechnol Adv* **2013**, *31*, 1374-1385.

(10) Issadore, D.; Park, Y. I.; Shao, H.; Min, C.; Lee, K.; Liong, M.; Weissleder, R.; Lee, H. Magnetic sensing technology for molecular analyses. *Lab on a Chip* **2014**, *14*, 2385-2397.

(11) Lai, L. M. H.; Goon, I. Y.; Chuah, K.; Lim, M.; Braet, F.; Amal, R.; Gooding, J. J. The Biochemiresistor: An Ultrasensitive Biosensor for Small Organic Molecules. *Angew Chem Int Edit* **2012**, *51*, 6456-6459.

(12) Di Corato, R.; Palumberi, D.; Marotta, R.; Scotto, M.; Carregal-Romero, S.; Gil, P. R.; Parak, W. J.; Pellegrino, T. Magnetic Nanobeads Decorated with Silver Nanoparticles as Cytotoxic Agents and Photothermal Probes. *Small* **2012**, *8*, 2731-2742.

(13) Chung, H. J.; Castro, C. M.; Im, H.; Lee, H.; Weissleder, R. A magneto-DNA nanoparticle system for rapid detection and phenotyping of bacteria. *Nat Nanotechnol* **2013**, *8*, 369-375.

(14) Le Sage, D.; Arai, K.; Glenn, D. R.; DeVience, S. J.; Pham, L. M.; Rahn-Lee, L.; Lukin, M. D.; Yacoby, A.; Komeili, A.; Walsworth, R. L. Optical magnetic imaging of living cells. *Nature* **2013**, *496*, 486-489.

(15) Leslie, D. C.; Li, J. Y.; Strachan, B. C.; Begley, M. R.; Finkler, D.; Bazydlo, L. A. L.; Barker, N. S.; Haverstick, D. M.; Utz, M.; Landers, J. P. New Detection Modality for Label-Free Quantification of DNA in Biological Samples via Superparamagnetic Bead Aggregation. *J Am Chem Soc* **2012**, *134*, 5689-5696.

(16) Ghosh, D.; Lee, Y.; Thomas, S.; Kohli, A. G.; Yun, D. S.; Belcher, A. M.; Kelly, K. A. M13-templated magnetic nanoparticles for targeted in vivo imaging of prostate cancer. *Nat Nanotechnol* **2012**, *7*, 677-682.

(17) Østerberg, F. W.; Rizzi, G.; Donolato, M.; Bejhed, R. S.; Mezger, A.; Strömberg, M.; Nilsson, M.; Strømme, M.; Svedlindh, P.; Hansen, M. F. On-Chip Detection of Rolling Circle

Amplified DNA Molecules from Bacillus Globigii Spores and Vibrio Cholerae. *Small* **2014**, *10*, 2877-2882.

(18) Kelley, S. O.; Mirkin, C. A.; Walt, D. R.; Ismagilov, R. F.; Toner, M.; Sargent, E. H. Advancing the speed, sensitivity and accuracy of biomolecular detection using multi-length-scale engineering. *Nat Nanotechnol* **2014**, *9*, 969-980.

(19) Hahn, Y. K.; Park, J. K. Versatile immunoassays based on isomagnetophoresis. *Lab on a Chip* **2011**, *11*, 2045-2048.

(20) Issadore, D.; Chung, H. J.; Chung, J.; Budin, G.; Weissleder, R.; Lee, H. mu Hall Chip for Sensitive Detection of Bacteria. *Adv Healthc Mater* **2013**, *2*, 1224-1228.

(21) Morozov, V. N.; Groves, S.; Turell, M. J.; Bailey, C. Three minutes-long electrophoretically assisted zeptomolar microfluidic immunoassay with magnetic-beads detection. *J Am Chem Soc* **2007**, *129*, 12628-12629.

(22) Morozov, V. N.; Morozova, T. Y. Electrophoresis-assisted active immunoassay. *Anal Chem* **2003**, *75*, 6813-6819.

(23) Tekin, H. C.; Cornaglia, M.; Gijs, M. A. M. Attomolar protein detection using a magnetic bead surface coverage assay dagger. *Lab on a Chip* **2013**, *13*, 1053-1059.

(24) Cornaglia, M.; Trouillon, R.; Tekin, H. C.; Lehnert, T.; Gijs, M. A. M. Magnetic Particle-Scanning for Ultrasensitive Immunodetection On-Chip. *Anal Chem* **2014**, *86*, 8213-8223.

(25) Shlyapnikov, Y. M.; Shlyapnikova, E. A.; Simonova, M. A.; Shepelyakovskaya, A. O.; Brovko, F. A.; Komaleva, R. L.; Grishin, E. V.; Morozov, V. N. Rapid Simultaneous Ultrasensitive Immunodetection of Five Bacterial Toxins. *Anal Chem* **2012**, *84*, 5596-5603.

(26) Orlov, A. V.; Khodakova, J. A.; Nikitin, M. P.; Shepelyakovskaya, A. O.; Brovko, F. A.; Laman, A. G.; Grishin, E. V.; Nikitin, P. I. Magnetic Immunoassay for Detection of Staphylococcal Toxins in Complex Media. *Anal Chem* **2013**, *85*, 1154-1163.

(27) Yellen, B. B.; Erb, R. M.; Son, H. S.; Hewlin, J. R.; Shang, H.; Lee, G. U. Traveling wave magnetophoresis for high resolution chip based separations. *Lab on a Chip* **2007**, *7*, 1681-1688.

(28) Gao, L.; Gottron, N. J.; Virgin, L. N.; Yellen, B. B. The synchronization of superparamagnetic beads driven by a micro-magnetic ratchet. *Lab on a Chip* **2010**, *10*, 2108-2114.

(29) Gao, L.; Tahir, M. A.; Virgin, L. N.; Yellen, B. B. Multiplexing superparamagnetic beads driven by multi-frequency ratchets. *Lab on a Chip* **2011**, *11*, 4214-4220.

(30) Lim, B.; Reddy, V.; Hu, X.; Kim, K.; Jadhav, M.; Abedini-Nassab, R.; Noh, Y.-W.; Lim, Y. T.; Yellen, B. B.; Kim, C. Magnetophoretic circuits for digital control of single particles and cells. *Nat Commun* **2014**, *5*.

(31) Gunnarsson, K.; Roy, P. E.; Felton, S.; Pihl, J.; Svedlindh, P.; Berner, S.; Lidbaum, H.; Oscarsson, S. Programmable motion and separation of single magnetic particles on patterned magnetic surfaces. *Adv Mater* **2005**, *17*, 1730-1734.

(32) Johansson, L.; Gunnarsson, K.; Bijelovic, S.; Eriksson, K.; Surpi, A.; Göthelid, E.; Svedlindh, P.; Oscarsson, S. A magnetic microchip for controlled transport of attomole levels of proteins. *Lab on a Chip* **2010**, *10*, 654-661.

(33) www.usbmikroskop.se.

(34) Schneider, C. A.; Rasband, W. S.; Eliceiri, K. W. NIH Image to ImageJ: 25 years of image analysis. *Nat Meth* **2012**, *9*, 671-675.

(35) Abramoff, M. D., Magalhães, Paulo J., Ram, Sunanda J. Image processing with ImageJ *Biophotonics international* **2004**, *11*, 36-42.

(36) Hakkinen, H. The gold-sulfur interface at the nanoscale. *Nat Chem* **2012**, *4*, 443-455.

(37) Xue, Y. R.; Li, X.; Li, H. B.; Zhang, W. K. Quantifying thiol-gold interactions towards the efficient strength control. *Nat Commun* **2014**, *5*.

(38) Yellen, B. B.; Friedman, G. Programmable assembly of colloidal particles using magnetic microwell templates. *Langmuir* **2004**, *20*, 2553-9.

(39) Kaur, J.; Singh, K. V.; Schmid, A. H.; Varshney, G. C.; Suri, C. R.; Raje, M. Atomic force spectroscopy-based study of antibody pesticide interactions for characterization of immunosensor surface. *Biosens Bioelectron* **2004**, *20*, 284-93.

(40) Lee, G. U.; Chrisey, L. A.; Colton, R. J. Direct measurement of the forces between complementary strands of DNA. *Science* **1994**, *266*, 771-3.

(41) Tamanaha, C. R.; Mulvaney, S. P.; Rife, J. C.; Whitman, L. J. Magnetic labeling, detection, and system integration. *Biosens Bioelectron* **2008**, *24*, 1-13.

(42) Shen, J.; Li, Y.; Gu, H.; Xia, F.; Zuo, X. Recent development of sandwich assay based on the nanobiotechnologies for proteins, nucleic acids, small molecules, and ions. *Chem Rev* **2014**, *114*, 7631-77.

(43) Berg, H. C.; Purcell, E. M. Physics of Chemoreception. *Biophys J* **1977**, *20*, 193-219.

(44) Berg, O. G.; Vonhippel, P. H. Diffusion-Controlled Macromolecular Interactions. *Annu Rev Biophys Bio* **1985**, *14*, 131-160.

(45) Stenberg, M.; Nygren, H. Kinetics of Antigen-Antibody Reactions at Solid-Liquid Interfaces. *J Immunol Methods* **1988**, *113*, 3-15.

(46) Lausted, C.; Hu, Z. Y.; Hood, L. Quantitative Serum Proteomics from Surface Plasmon Resonance Imaging. Mol Cell Proteomics 2008, 7, 2464-2474.

(47) Akter, R.; Jeong, B.; Rahman, M. A. Stimulated mass enhancement strategy-based highly sensitive detection of a protein in serum using quartz crystal microbalance technique. Analyst 2015, 140, 995-8.

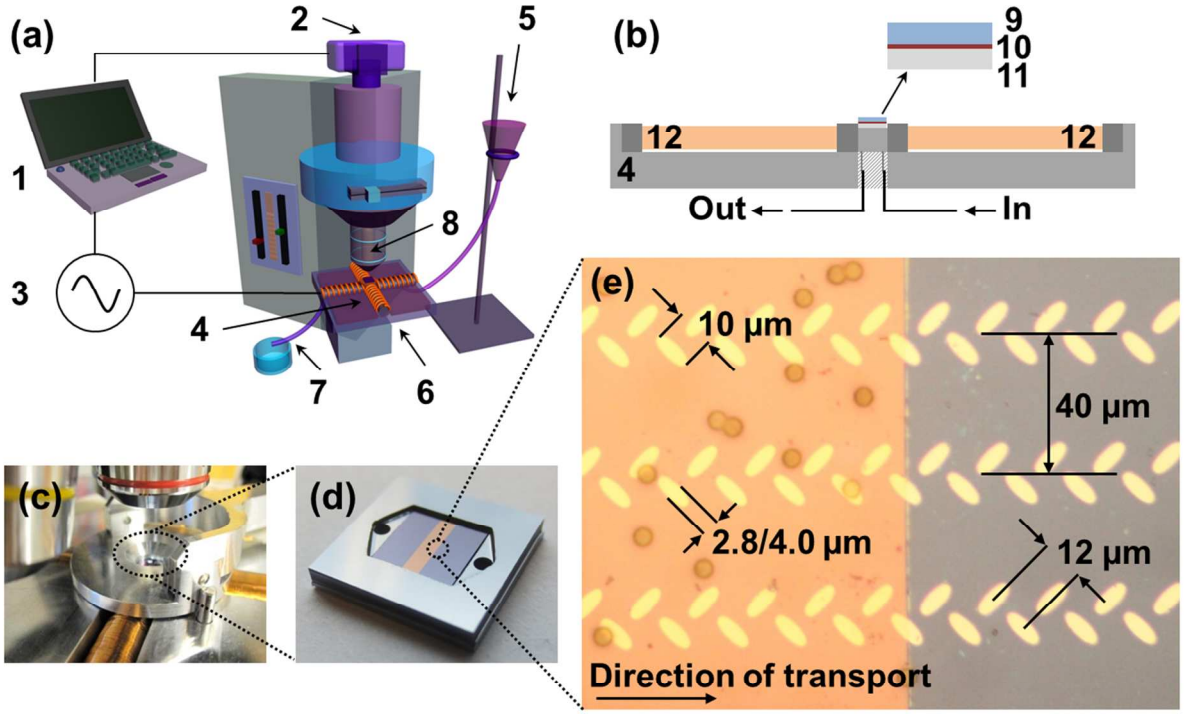

Scheme 1. (a) The experimental set-up. (1) is the computer, controlling a digital camera (2) and a power source (3). (4) is a platform holding two pairs of electromagnets and a fluid cell containing a thin film patterned microchip. (5) is the syphon reservoir, (6) is the inlet where the liquid enters the fluid cell and (7) is the outlet. (8) is an objective attached to an optical microscope. (b) A cross section of the platform (4) holding the magnets and the fluid cell. (9), (10), and (11) are the top part, a gasket and the bottom part of the fluid cell, respectively. (12) is the electromagnets. (c) A close-up of the arm keeping the top part of the fluid cell in place. (d) The bottom part of the fluid cell holding the microchip. (e) A colorized photomicrograph of the boundary between the detection area in gold (to the left) and the bare chip (to the right). The transport lines with magnetic thin film ellipses can be seen. On the detection area, also some 5 µm MBs can be seen.

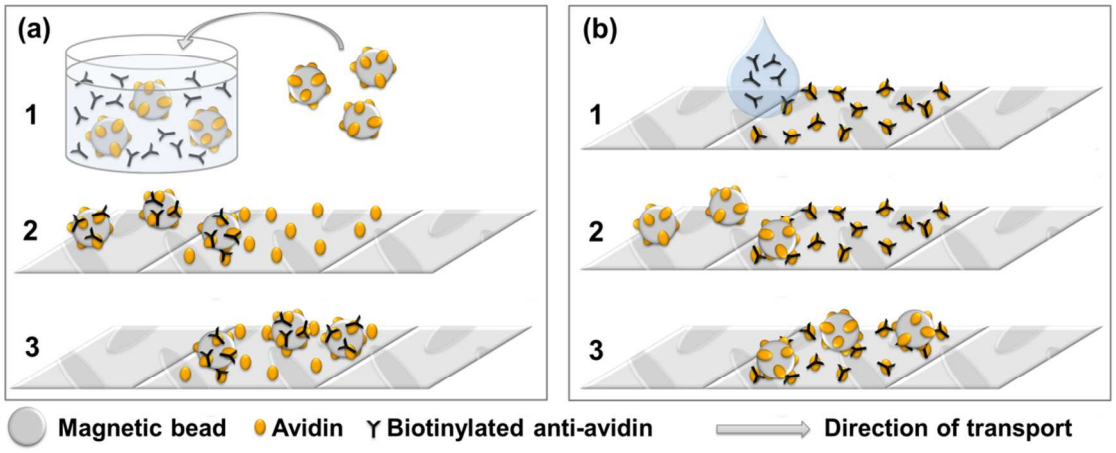

Figure 1. (a) A schematic illustration of a positive sample being analyzed using the off-chip approach. 1) MBs with capture molecules are subjected to a target antibody containing sample. 2) The MBs are transported across the chip functionalized with capture molecules. 3) After rinsing, MBs have been immobilized on the detection area by the target antibodies that act as cross-linkers. (b) A schematic illustration of a positive sample being analyzed using the on-chip labeling approach. 1) A target antibody containing droplet is pipetted onto the chip, the antibodies are immobilized by the capture molecules on the detection area. 2) MBs with capture molecules are transported across the chip. 3) After rinsing, MBs have been immobilized on the detection area by the target antibodies that act as cross-linkers.

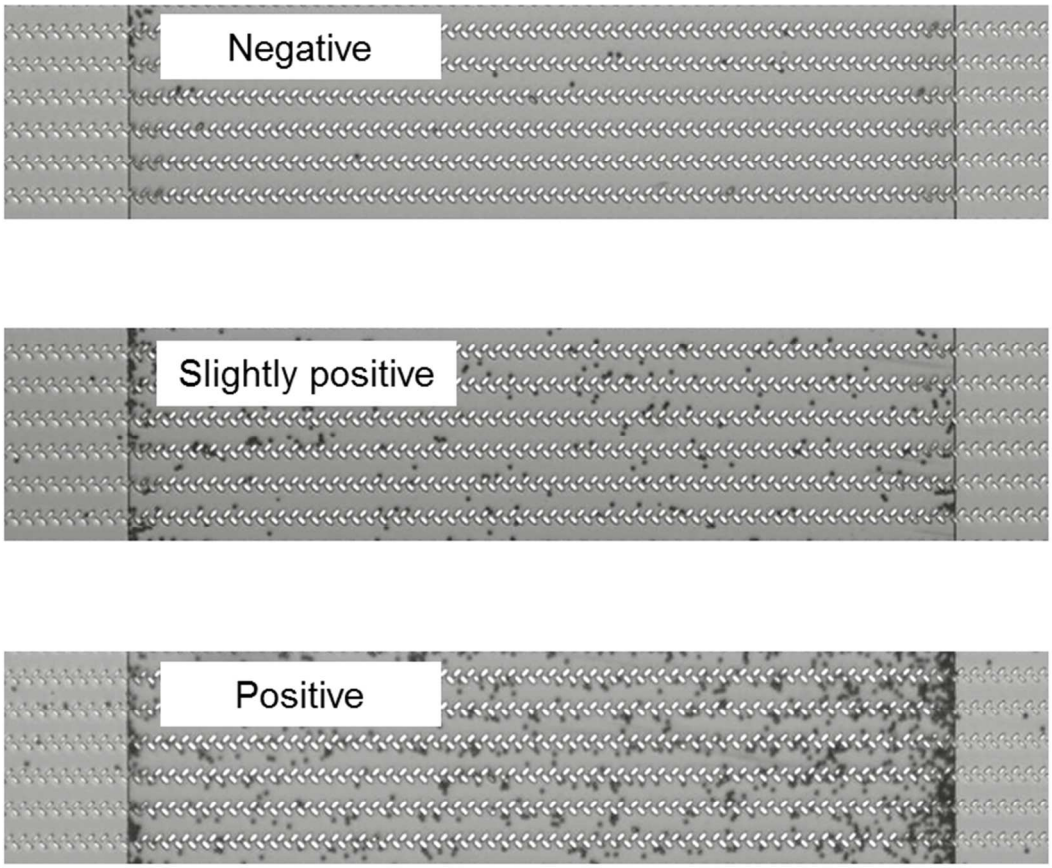

Figure 2. Photomicrographs, each showing approximately 1270×260 μm^2 of the detection area, displaying surface coverage results for a negative, a slightly positive (target concentration of around 1 ng/ml) and a positive (target concentration of around 1 μg/ml) sample.

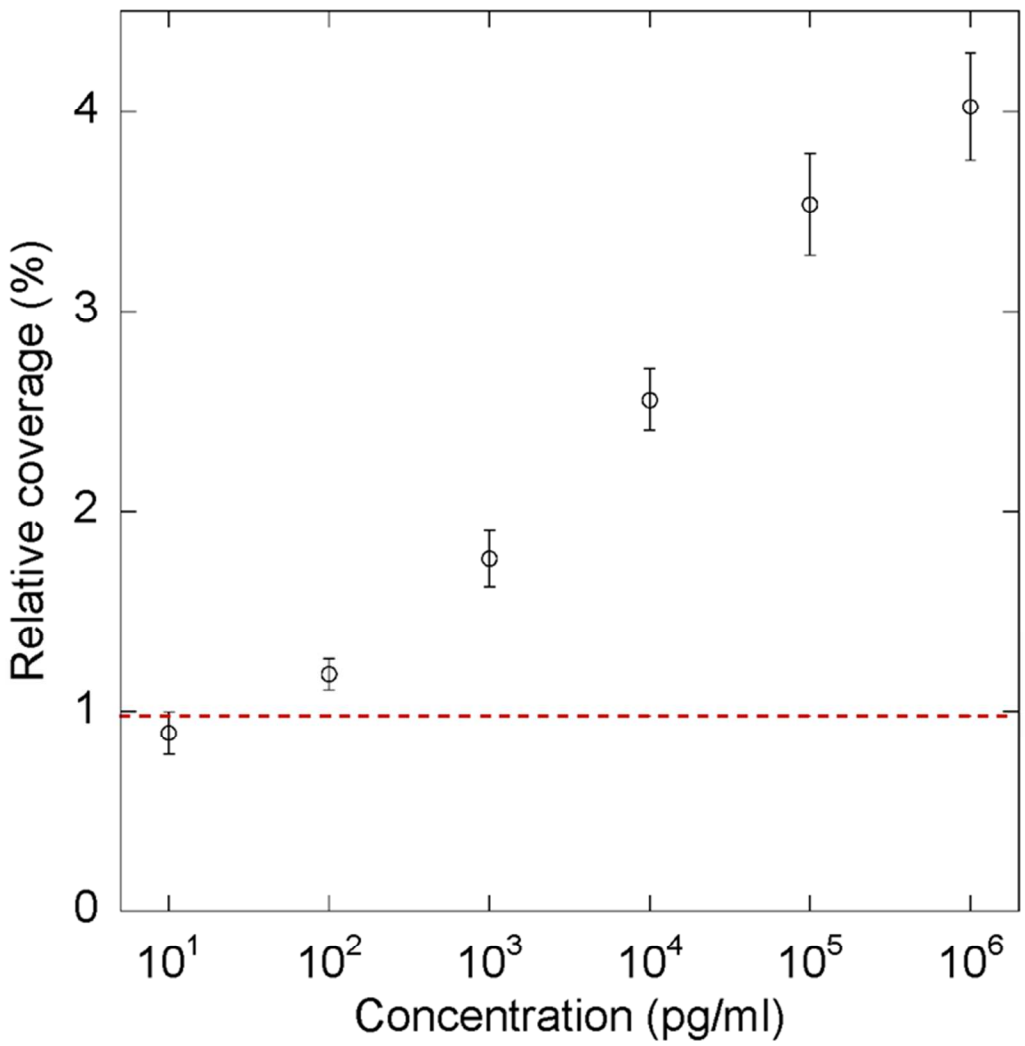

Figure 3. The results for a series of measurements performed using the off-chip labeling approach. A data point represents the average relative surface coverage of the three disposable chips and the error bars represent the standard deviations. The dashed line indicates the LOD.

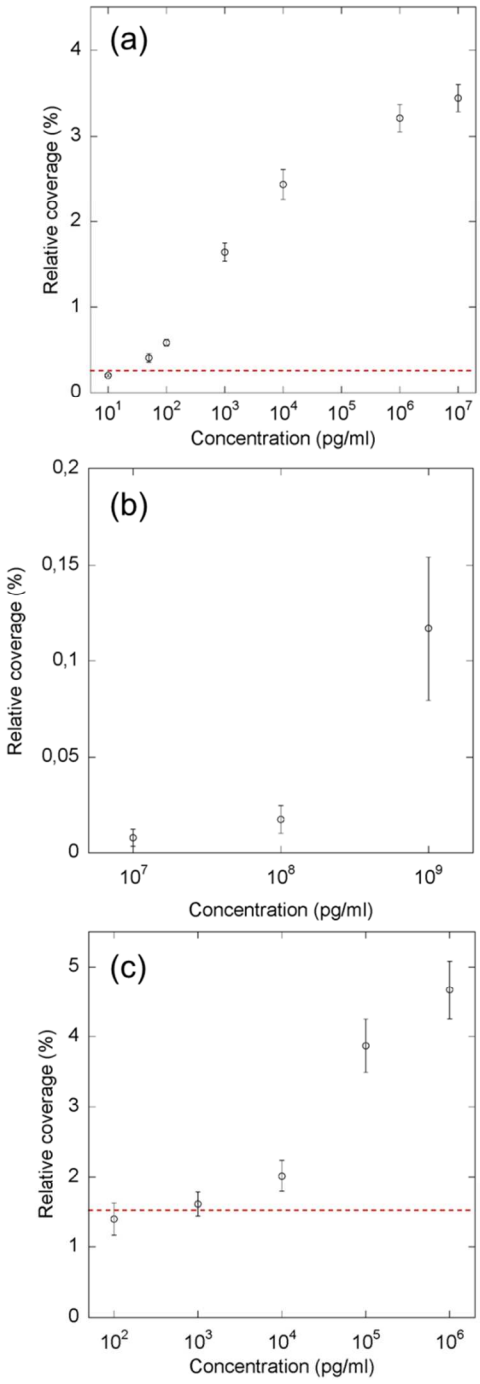

Figure 4. (a) The results for a series of measurements performed using the on-chip labeling approach. A data point represents the average relative surface coverage of the disposable three chips and the error bars represent the standard deviations. The dashed line indicates the LOD. (b) The results for three measurements performed using the on-chip labeling approach but without

applied magnetic field. Each concentration was measured three times using disposable chips and the presented results correspond to averages with error bars representing the standard deviations. (c) The results for a series of measurements performed using the on-chip labeling approach for samples in PBS + 10% serum. The three lower concentrations were measured three times and the two higher concentrations were measured two times, in all cases disposable chips were used. A data point represents the average surface coverage of the chips and the error bars represent the standard deviations. The dashed line indicates the LOD.

TOC Graphic